ADVANCES IN ATMOSPHERIC SCIENCES, VOL. 32, SEPTEMBER 2015, 1291–1302

Turbulence Intensity and Turbulent Kinetic Energy Parameters over a Heterogeneous Terrain of Loess Plateau

YUE Ping*, ZHANG Qiang, WANG Runyuan, LI Yaohui, and WANG Sheng

Key Laboratory of Arid Climatic Change and Reducing Deserter of Gansu Province, Institute of Arid Meteorology, China Meteorological Administration, Lanzhou 730020

(Received 19 November 2014; revised 02 March 2015; accepted 17 March 2015)

ABSTRACT

A deep understanding of turbulence structure is important for investigating the characteristics of the atmospheric boundary layer, especially over heterogeneous terrain. In the present study, turbulence intensity and turbulent kinetic energy (TKE) parameters are analyzed for different conditions with respect to stability, wind direction and wind speed over a valley region of the Loess Plateau of China during December 2003 and January 2004. The purpose of the study is to examine whether the observed turbulence intensity and TKE parameters satisfy Monin–Obukhov similarity theory (MOST), and analyze the wind shear effect on, and thermal buoyancy function of, the TKE, despite the terrain heterogeneity. The results demonstrate that the normalized intensity of turbulence follows MOST for all stability in the horizontal and vertical directions, as well as the normalized TKE in the horizontal direction. The shear effect of the wind speed in the Loess Plateau region is strong in winter and could enhance turbulence for all stability conditions. During daytime, the buoyancy and shear effect together constitute the generation of TKE under unstable conditions. At night, the contribution of buoyancy to TKE is relatively small, and mechanical shearing is the main production form of turbulence.

Key words: heterogeneous terrain, turbulence intensity, turbulent kinetic energy, Monin–Obukhov similarity function

Citation: Yue, P., Q. Zhang, R. Y. Wang, Y. H. Li, and S. Wang, 2015: Turbulence intensity and turbulent kinetic energy parameters over a heterogeneous terrain of the Loess Plateau, China. *Adv. Atmos. Sci.*, **32**(9), 1291–1302, doi: 10.1007/s00376-015-4258-9.

1. Introduction

Turbulent transport is one of the most important characteristics of the atmospheric boundary layer. The exchange of momentum, heat, water and other substances between land and atmosphere mainly takes place in the form of turbulent diffusion (Louis, 1979; Powell et al., 2003; Martins et al., 2009; Mahrt, 2010). Therefore, the characteristics of the atmospheric turbulence near-surface layer become the important characterization parameters of the land–atmosphere interaction (Monin and Yaglom, 1971; Louis, 1979; Teixeira et al., 2008). An accurate description of the land–atmosphere turbulence exchange process depends on the understanding of the characteristics of atmospheric turbulence (Muschinski et al., 2004; Acevedo et al., 2007; Teixeira et al., 2008). However, it is clear that, for atmosphere turbulent flows, we cannot directly describe the exchange process (Massman and Lee, 2002; Moraes et al., 2005). Instead, previous studies (Nieuwstadt, 1984; Sorbjan, 1987) have concentrated on understanding the statistical properties of atmosphere turbulence.

Many observational experiments have demonstrated that the relationship between turbulence intensity and atmospheric stability, determined according to Monin–Obukhov similarity theory (MOST), can effectively describe the characteristics of the turbulent exchange over a uniform homogeneous underlying surface (Businger et al., 1971; Nieuwstadt, 1984; Sorbjan, 1987). However, the complexity and diversity of the earth's surface brings tremendous difficulties and challenges to the understanding of the turbulence exchange processes between land and atmosphere (Kaimal, 1973; Panofsky et al., 1977; Li et al., 2003; Hammerle et al., 2007). The turbulent exchange of an inhomogeneous underlying surface is not only related to the characteristics of the land surface, but also the changes of turbulence intensity itself (Mahrt et al., 1998; Mahrt, 2007). Currently, the parameterization of heterogeneous or complex underlying turbulence is recognized as one of the most difficult problems in the micrometeorology research field (Mahrt et al., 1998; Andreas and Hicks, 2000; Moraes, 2000; Al-Jiboori et al., 2001). For complex terrain, Moraes et al. (2005) showed σ_u/u_* and σ_v/u_* that dependence with z/L just for wind speed higher than the threshold $U > 1$ m s^{-1} and $-1 \leqslant z/L \leqslant 0$ (where, σ is the standard deviation of velocity, u_* is the friction velocity, z/L is the stability parameter, in which z is the height of the

* Corresponding author: YUE Ping
Email: jqyueping@126.com

sensor above the ground and $L = -u_*^3\overline{T_v}/kg(\overline{w'T_v'})$, $\overline{T}_v$ is the mean virtual temperature, κ is the Karman constant, g is the acceleration due to gravity, and $\overline{w'T_v'}$ is turbulent heat flux). Martins et al. (2009) found that both of the parameters σ_u/u_* and σ_v/u_* follow MOST in convective and stable conditions for a limited range of z/L.

As a globally unique and important geographical region, the Loess Plateau of China is an important part of the country's arid and semi-arid landscape, and the heterogeneity of the land surface is obvious (Huang et al., 2008; Yue et al., 2011). The region features a gully–hilly crisscross pattern, and the underlying surface is highly undulating. Therefore, the turbulence characteristics of the region are complicated, while the turbulent transport is more typical (Huang et al., 2008; Yue et al., 2012; Zhang et al., 2013). There are significant differences in the resulting turbulence characteristics, even at the same observation station, when airflow from different directions passes the observation point. This is because of the different characteristics of the underlying surfaces and the "memories" they impose (Martins et al., 2009; Liu et al., 2012).

In fact, the factors affecting the inhomogeneity of the underlying surface of the Loess Plateau are not only topographic; the complexity of the vegetation in the region is also regarded as a very important non-uniform factor (Zhang et al., 2013). However, changes in wind speed in the surface layer will also affect the structure and morphology of this kind of roughness element, even when the underlying surface conditions are exactly the same. Thus, the dynamic roughness size can change (Yue et al., 2013; Zhang et al., 2013), which makes it even more challenging to understand the regional characteristics of turbulent flow. To eliminate the influence of the underlying surface vegetation on the characteristics of turbulence, bare soil data for the winter season are used in the present study. To analyze the effects of topographic heterogeneity on the characteristics of turbulence, the wind direction and wind speed at the observation site are classified, and verify the applicability of MOST in research on the complex underlying surface of the Loess Plateau. In addition, the effects of shear and buoyancy contribution on turbulent kinetic energy (TKE) are studied through the classification of wind directions.

The remainder of the paper is structured as follows: First, the observational data and the parameterization of turbulence intensity are introduced in section 2. In section 3, the statistical characteristics of TKE and the contribution of shear and buoyancy to TKE are analyzed. Conclusions are presented in section 4.

2. Material and Methods

2.1. *Observations*

The observations were made in a valley region of Dingxi, over the Loess Plateau in Northwest China [(35°35′N, 104°37′E), elevation: 1896.7 m above sea level; Fig. 1a maps the topography of the study area, and Fig. 1b is a photograph of the flux observation station]. The research area belongs to a semi-arid climate region, with an annual average temperature of 6.3°C, average annual precipitation of 419 mm, annual average wind speed of 1.8 m s^{-1}, and average annual sunshine of 2500 hours. The maximum potential evaporation is greater than 1526 mm.

The observational data for December 2003 to January 2004 provide half-hour records of velocity from a sonic anemometer (CSAT3, Campbell Scientific, USA) located at height $z = 2$ m on the northern side of a 20 m tower. The sonic anemometer is aligned with local gravity and its boom is directed north. The three wind velocity components and virtual temperature are sampled at 10 Hz. Basic quality control of the raw 10 Hz data involve the detection of "soft" and "hard" spikes (Vickers and Mahrt, 1997; Schmid et al., 2003; Zuo

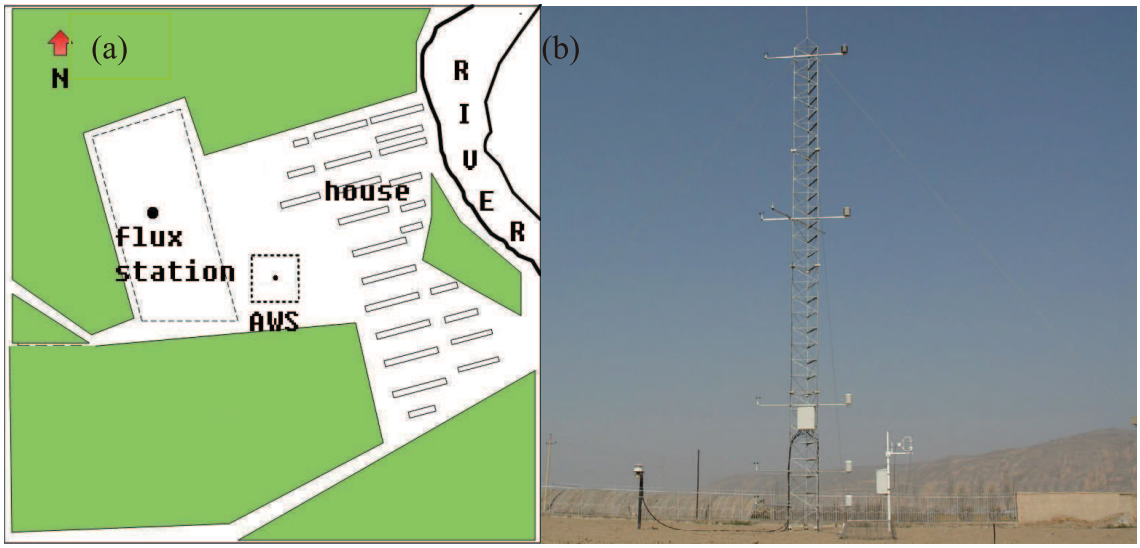

Fig. 1. (a) Topographical map; (b) the flux observation station.

et al., 2009; Liu et al., 2012). Half-hour records occurring during precipitation, and runs with frictional velocity (u_*) of $\leqslant 0.01$ m s^{-1}, are rejected (Song et al., 2010). Following the above screening process, we have available to us 320 simultaneous samples averaged for 30 min to stable stratification, and 445 samples averaged for 30 min to unstable atmospheric stratification.

Figure 2 shows that the most frequent wind direction range are 105°–150° (southeast) and 285°–310° (west-northwest). Houses with different low heights of 3–5 m are distributed about 100 m away from the southeast direction of the observation station. There is relatively flat open land to the northwest, with a length of about 500 m and width of 300 m, without tall buildings and trees. Table 1 presents the prevailing wind direction aerodynamic roughness length and friction velocity at the Dingxi site for different stability conditions.

2.2. *Turbulence flux source areas*

To analyze the effects of the inhomogeneity of the topography on the characteristics of turbulence, the Flux Source Area Model (FSAM) (Schmid, 1994) is selected in the present study to calculate the distribution of the turbulent flux source areas of Dingxi under different stability conditions in the dominant wind directions (Fig. 3). The location of the observation point is used as the origin. The direction opposite to the horizontal wind speed is used as the *x*-axis. The direction perpendicular to the *x*-axis direction is used as the *y*-axis. When the contribution of the flux source area at the observation height of 2 m at Dingxi station reaches 90%: (1) In the southeast direction, a, d, e and X_m (where X_m is the maximum source location, i.e., the upwind distance of the surface element with the maximal effect on a given sensor; a is the distance from the near end of the area to the sensor; e is the distance from the far near end of the area to the sensor (Schmid, 1994); and d is the maximum lateral half-width of the source area), under conditions of stable atmospheric stratification, are 9.9, 22.8, 71.4 m and 21.7 m, respectively. Under neutral conditions their values are 12.4, 29.3, 99.3 m and 27.9 m, respectively, and under unstable conditions they are 13.6, 32.2, 114.9 m and 31.4 m, respectively. (2) In the west-northwest direction, under conditions of stable atmospheric stratification, a, d, e and X_m are 10.1, 20.4, 75.0 m and

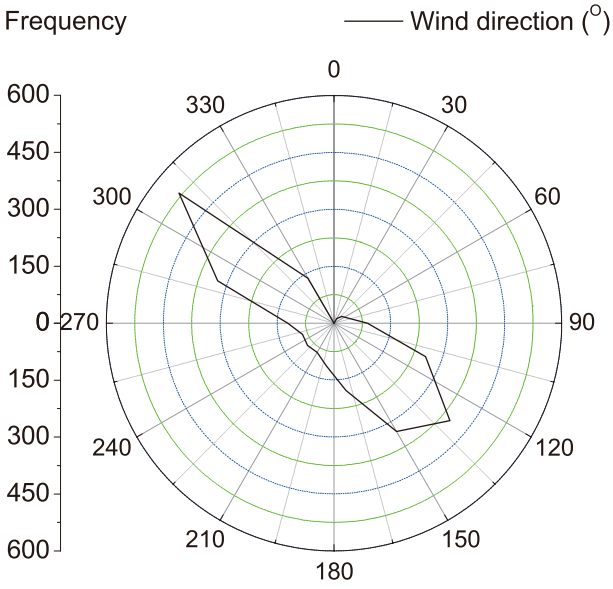

Fig. 2. Wind rose at the 2 m level for the Dingxi site from December 2003 to January 2004.

Table 1. Aerodynamic roughness and friction velocity in different wind directions.

	Z_0 (m)				U_* (m s^{-1})			
Wind direction (°)	Unstable	Neutral	Stable	Mean	Unstable	Neutral	Stable	Mean
105–150	0.023	0.032	0.047	0.033	0.115	0.158	0.072	0.110
285–310	0.026	0.033	0.031	0.030	0.218	0.225	0.151	0.182

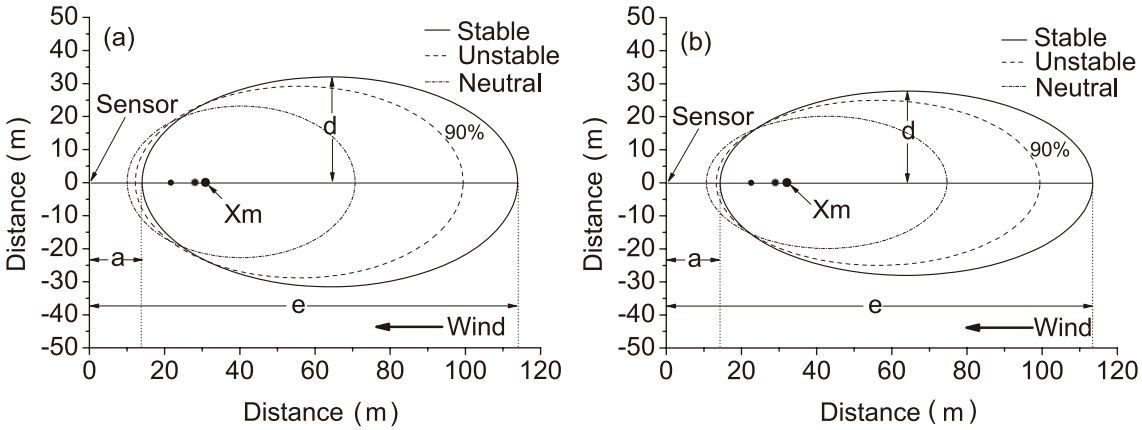

Fig. 3. Turbulent source areas in the prevailing direction under different stability conditions.

22.4 m, respectively; under neutral conditions they are 12.8, 25.0, 99.6 m and 28.6 m, respectively; and under unstable conditions they are 14.0, 27.4, 114.6 m and 28.6 m, respectively. This shows that the contributing ranges of flux source area in the dominant wind direction are as follows: stable conditions > neutral conditions > unstable conditions. At the same time, the tensile range in the crosswind direction of the flux source area in the direction of southeast wind is significantly greater than that in the west-northwest direction, and this difference is mainly caused by topography.

3. Results

3.1. *Normalized standard deviation of the velocity fluctuations*

The normalized velocity variance component of wind speed reflects the turbulence intensity, and it can effectively describe TKE and turbulent transport characteristics of the planetary boundary layer (Martins et al., 2009). According to MOST, the variance of near-surface layer wind speed can be expressed by the universal function $\phi_x(z/L)$ of the stability parameter (z/L) in horizontally homogeneous and steady flow after it is nondimensionalized by the characteristic scale parameter [i.e., $\phi_x(z/L) = \sigma_i/u_* = c_1(1 \pm c_2 z/L)^{c_3}$, where c_1, c_2, and c_3 are universal constants] (Businger et al., 1971; Nieuwstadt, 1984; Sorbjan, 1987). Many experimental results (Panofsky and Dutton, 1984; Al-Jiboori et al., 2001; Martins et al., 2009) have shown that the nondimensional velocity variance with z/L agrees with the 1/3 power law under unstable stratification conditions. However, there is no agreement on the behavior of σ_w/u_* with z/L, even for flat terrain, such as the Kansas experiment (Nieuwstadt, 1984; Panofsky and Dutton, 1984; Smedman, 1988). There are two possible reasons for this phenomenon: One view is that the orders of σ_i/u_* and z/L themselves are relatively small when the stratification is stable; plus, there are also many uncertainties relating to the turbulent velocity variance itself (Panofsky and Dutton, 1984). Another view is that the dimensionless turbulence velocity component is almost unrelated to the atmospheric stability under weakly stable conditions (Nieuwstadt, 1984; Smedman, 1988).

In theory, the difference in the topography of uniform terrain and the density and structure of the roughness length and other physical properties is very small, meaning the turbulence can be regarded as isotropic, and the impact of changes in wind direction on the characteristics of turbulence can be ignored (Zhang et al., 2013). However, observational results (Nieuwstadt, 1984; Smedman, 1988; Martins et al., 2009; Liu et al., 2012) indicate that the constant values of the normalized speed variances with z/L and $\phi_x(z/L)$ also have significant differences, because of the different underlying surface vegetation states, even under conditions of uniform terrain. For complex terrain, the effects of topography on turbulence characteristics cannot be ignored (Panofsky et al., 1977; Founda et al., 1997; Martins et al., 2009). Figures 4 and 5 present the changes in σ_u/u_*, σ_v/u_* and σ_w/u_* with z/L according to the southeast and west-northwest wind directions at Dingxi. Equations (1–3) and (4–6) are the optimal universal functions in the southeast and west-northwest directions, respectively:

$$\sigma_u/u_* = \begin{cases} 3.7(1-3.2z/L)^{1/3} & z/L<0 \\ 3.7(1+5.8z/L)^{1/3} & z/L>0 \end{cases}, \quad (1)$$

$$\sigma_v/u_* = \begin{cases} 3.3(1-3.4z/L)^{1/3} & z/L<0 \\ 3.3(1+8.6z/L)^{1/3} & z/L>0 \end{cases}, \quad (2)$$

$$\sigma_w/u_* = \begin{cases} 1.3(1-2.8z/L)^{1/3} & z/L<0 \\ 1.3(1+3.8z/L)^{1/3} & z/L>0 \end{cases}, \quad (3)$$

$$\sigma_u/u_* = \begin{cases} 2.9(1-3.6z/L)^{1/3} & z/L<0 \\ 2.9(1+6.2z/L)^{1/3} & z/L>0 \end{cases}, \quad (4)$$

$$\sigma_v/u_* = \begin{cases} 3.2(1-5.3z/L)^{1/3} & z/L<0 \\ 3.2(1+7.3z/L)^{1/3} & z/L>0 \end{cases}, \quad (5)$$

$$\sigma_w/u_* = \begin{cases} 1.4(1-3.1z/L)^{1/3} & z/L<0 \\ 1.4(1+4.6z/L)^{1/3} & z/L>0 \end{cases}. \quad (6)$$

The observations indicate that σ_u/u_*, σ_v/u_* and σ_w/u_* in the semi-arid region of the Loess Plateau are functions of z/L under convective conditions and follow a 1/3 power law, and that the dispersion in the vertical direction is smaller than that in the horizontal direction. Founda et al. (1997), Al-Jiboori et al. (2001), Moraes et al. (2005), Martins et al. (2009) and Liu et al. (2012) reported that, under convective conditions, σ_w/u_* behaves similarly to that over flat terrain. Zhang et al. (2001) also found that the values of σ_w/u_* tend to follow similarity relations, irrespective of the terrain, under unstable conditions. According to Panofsky and McCormick (1960), the σ_w is connected with the rates of shear and buoyant production of TKE. Because the turbulent exchange in the vertical direction is stronger and the turbulent adaptability is faster, the difference of the variance of velocity σ_w/u_* in different wind directions is relatively small. The differences of the ratio in the horizontal direction are more obvious, which is mainly caused by the heterogeneity of the underlying surface at the observation station. Panofsky and Dutton (1984) hypothesized that, over heterogeneous terrain, the vertical fluctuations near the surface layer are produced by small-scale eddies that rapidly adjust to the terrain changes, and their hypothesis was verified by Moraes et al. (2005) and Martins et al. (2009) for convective and weakly stable conditions.

Recent studies show that, for stable conditions, σ_u/u_*, σ_v/u_* and σ_w/u_* satisfy the 1/3 power law. Theoretically, the atmospheric turbulence will be restricted when the atmospheric stratification is stable, so the standard deviation of wind velocity will decrease with z/L increasing. However, many observational results have demonstrated that the standard deviation of wind velocity increases with the enhanced atmospheric stability (Ma et al., 2002; Yue et al., 2011). This is because intermittent turbulence and other movements may be triggered when the atmospheric stability of the boundary layer increases to a certain extent (Zeri and Sá, 2011). The results reported by Al-Jiboori et al. (2001) and Moraes et al.

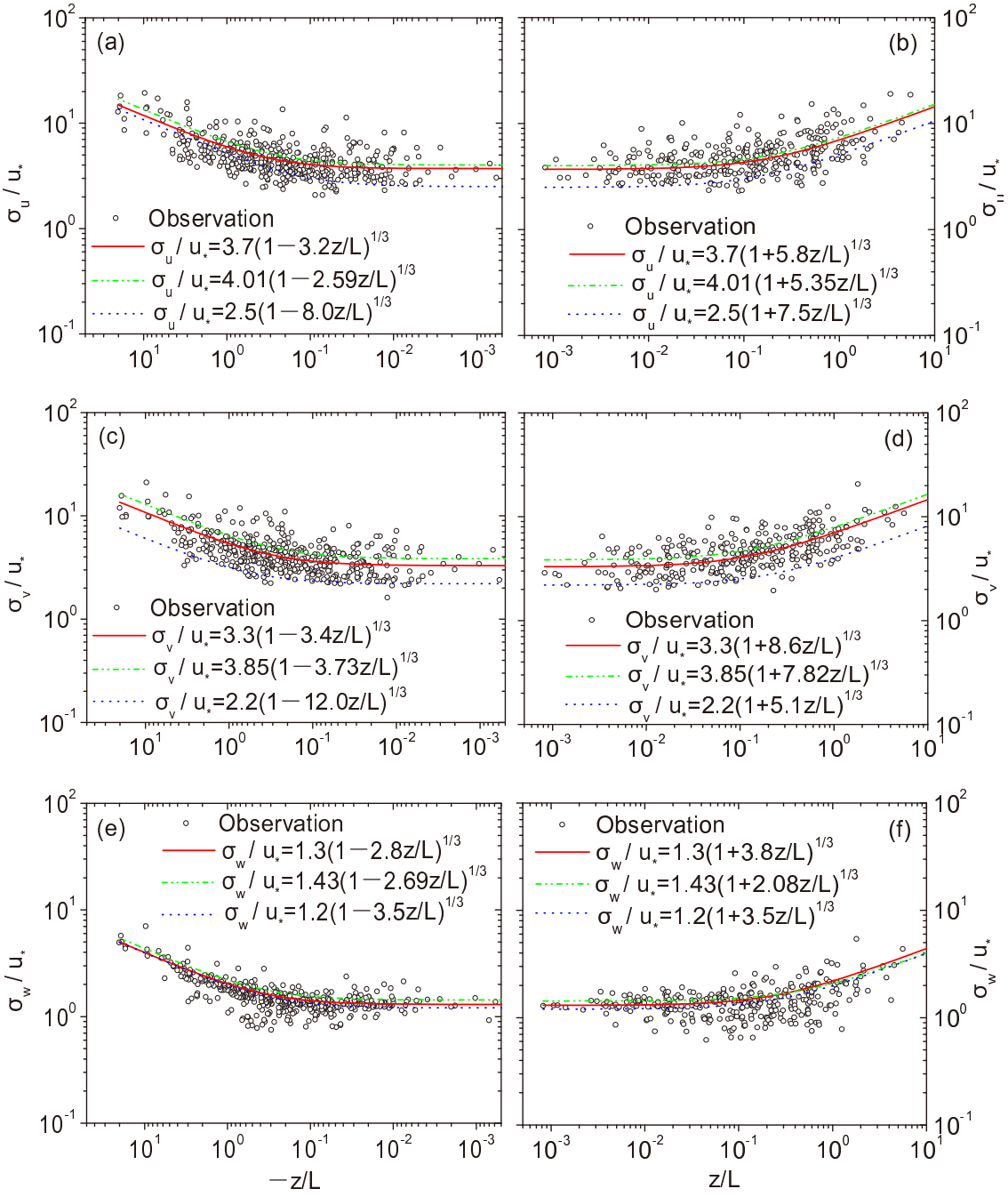

Fig. 4. Dimensionless wind velocity variance at Dingxi with stability (southeast direction).

(2005) showed that the ratio of σ_w/u_*, under stable conditions, increases slightly with stability—a finding later verified by Martins et al. (2009), only for $0 \leqslant z/L \leqslant 1.5$.

In the near-neutral regime, the differences of the normalized standard deviation of wind speed in different directions are significant, although the values for Dingxi are approximately equal to a constant (Table 2). In the southeast direction, $\sigma_u/u_* > \sigma_v/u_* > \sigma_w/u_*$. In the west-northwest direction, $\sigma_v/u_* > \sigma_u/u_* > \sigma_w/u_*$. Compared with previous experimental results of near-neutral conditions, the difference of the turbulence intensity in the horizontal direction is obvious, but the vertical difference is small (Ma et al., 2002; Yue et al., 2011). Table 3 shows the normalized standard deviation of velocity components under near-neutral stratification for different areas. The values of normalized standard deviation of velocity components are larger than those reported for other areas of flat terrain, and they are close to the values of rough mountain terrain reported by Mahrt et al. (1998). From Table 3 it can be concluded that the values of horizontal normalized standard deviation of velocity increase with increasing surface roughness. However, it is difficult to perform a quantitative analysis because of the

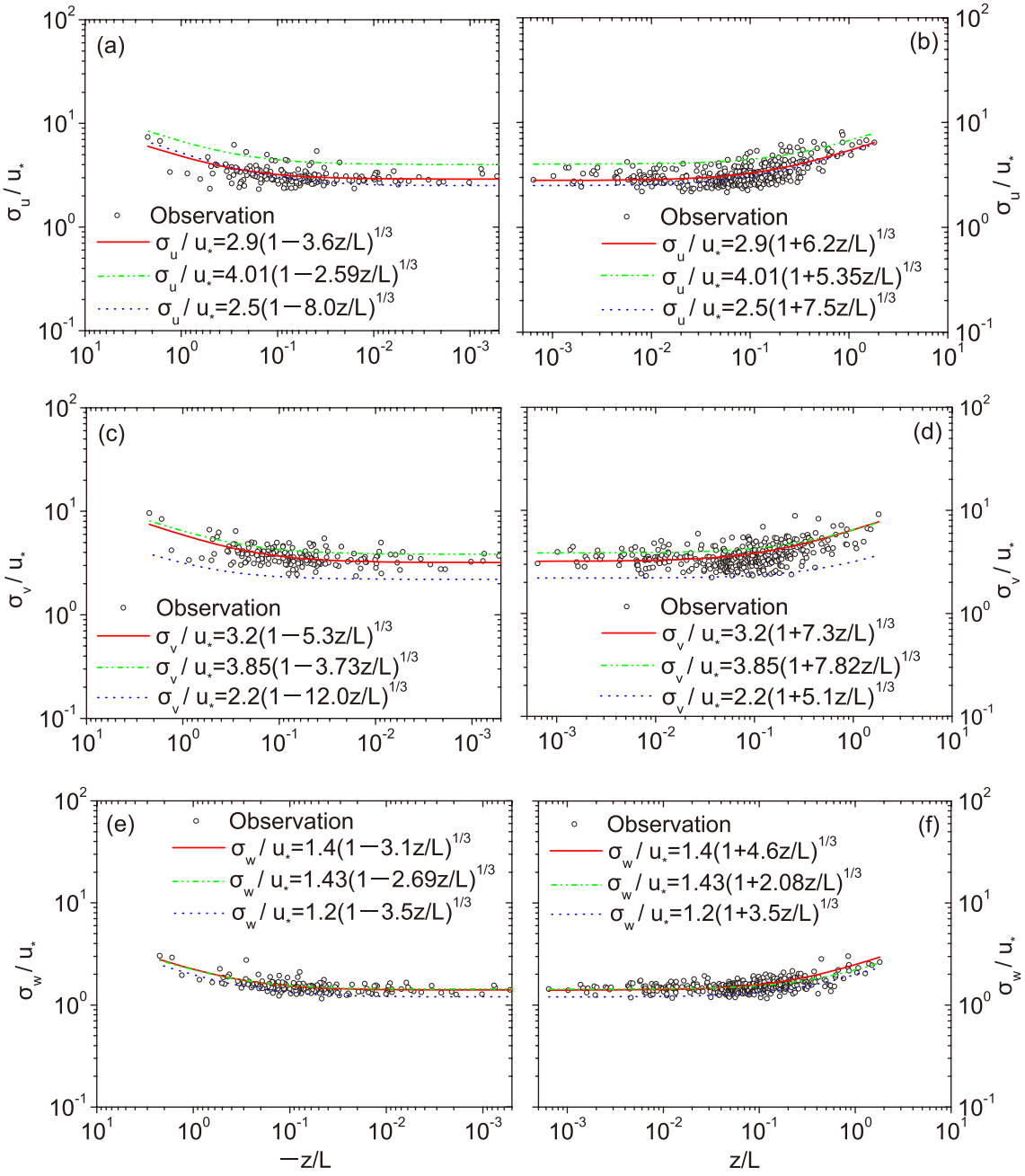

Fig. 5. Dimensionless wind velocity variance at Dingxi with stability (west-northwest direction).

Table 2. Aerodynamic roughness and normalized standard deviation of wind speed.

Wind direction (°)	Z_0 (m)	σ_u/u_*	σ_v/u_*	σ_w/u_*
105–150	0.033	3.7	3.3	1.3
285–310	0.030	2.9	3.2	1.4

differences in the terrain and vegetation, nonturbulent airflow movement, observational apparatus error, and sensor height (Panofsky and Dutton, 1984; Zeri and Sá, 2011). In particular, according to Wilson (2008), the effects of the definition and estimation of friction velocity cannot be ignored. Across the population of estimates of neutral σ_i/u_*, inconsistencies exist in the estimation of u_*, because some early measurement campaigns lacked an instrument capable of measuring the shear directly (the two common definitions for u_* are $u_{*A}^4 = (\overline{u'w'})^2 + (\overline{v'w'})^2$ and $u_{*B} = \sqrt{|\overline{u'w'}|}$). Obviously, $u_{*A} > u_{*B}$, and, if chosen for normalization, must boost σ_i/u_* relative to the alternative choice.

Interestingly, the normalized standard deviation of vertical velocity of the Loess Plateau at Dingxi is very close to that of the observational results of the Qinghai–Tibetan Plateau (Ma et al., 2002) and the Mongolian Plateau (Yue et al., 2011). Al-Jiboori et al. (2001), Zhang et al. (2001) and Moraes et al. (2005) also showed the normalized standard deviation of vertical velocity over complex topography to be

Table 3. Standard deviation of the velocity over difference land surfaces for neutral stratification conditions.

Source	σ_u/u_*	σ_v/u_*	σ_w/u_*	Underlying surface
Panosfky and Dutton (1984)	3.20	2.90	1.25	Flat surface
Panosfky and Dutton (1984)	2.39	1.92	1.24	Rough terrain
Mahrt et al. (1998)	3.50	3.80	1.24	Rough mountain terrain
Mahrt et al. (1998)	2.45	1.90	1.25	Plains
Niu et al. (2012)	3.73	3.49	1.62	Nanjing suburb
Ma et al. (2002)	4.01	3.85	1.43	Tibetan Plateau
Yue et al. (2011)	2.50	2.20	1.20	Inner Mongolia grassland
Liu et al. (2003)	2.90	2.90	1.45	Wandering dune
This study	3.30	3.25	1.35	Rough terrain of Loess Plateau

close to that of uniform terrain for unstable conditions. Figures 4 and 5 present the function between $\sigma_i/u_*(i = v,v,w)$ and z/L of our dataset and the Qinghai–Tibetan Plateau and Mongolian Plateau for comparison purposes. The results show that the σ_u/u_* and σ_v/u_* of the Loess Plateau at Dingxi are less than those of the Qinghai Tibetan Plateau, but larger than those of the Mongolian Plateau, which agrees with the notion that the topographic effects on horizontal wind speed are substantial. From the general topographic characteristics of the Qinghai–Tibetan Plateau, the Loess Plateau and the Mongolia Plateau, the topographic relief of the Qinghai–Tibetan Plateau is more marked than that of the Loess Plateau, and the changes of the terrain on the Loess Plateau are more prominent to those of the relatively flat Mongolia Plateau (Ma et al., 2002; Yue et al., 2011). From the results of the two prevailing wind directions at Dingxi, the difference in the normalized standard deviation of horizontal velocity is significant. The wind velocity fluctuation in the horizontal direction is mainly produced by quasi horizontal turbulence with relatively large scale, and its typical scale is generally several hundred meters or more, meaning its adaptability to the changes in terrain is slow.

3.2. *Effects of horizontal wind speed on normalized standard deviation*

Moraes et al. (2005) found that, for unstable conditions, there is good correlation between σ_u/u_* and σ_v/u_* and z/L, but only when the wind speed over the complex underlying surface is greater than a threshold ($U > 1$ m s^{-1}). Therefore, the variances of the horizontal wind components are influenced by large convective cells. Anfossi et al. (2005) found that there is a tendency for slightly higher values of σ_v/u_* with increasing stability for stable conditions over complex terrain. Figures 6 and 7 present the change of turbulent intensity with atmospheric stability in the southeast and west-northwest wind directions under different wind speed conditions at the Dingxi site. There is a close connection between σ_u/u_*, σ_v/u_* and σ_w/u_* with z/L for all stability conditions, and the variances of the turbulence intensity are affected by the horizontal wind speed. Under unstable conditions, the decreasing trend of turbulence intensity with stability increases more significantly under the conditions of high speed wind than low speed wind. Under stable conditions, the increasing trend of turbulence intensity with stability increases more significantly under the conditions of high speed wind than low speed wind. The characteristics are consistent with the results of Martins et al. (2009).

3.3. *Statistical characteristics of TKE*

TKE is a measure of turbulence intensity, and it is one of the most important variables in micrometeorology (Niu et al., 2012). TKE involves the transfer of momentum, heat and moisture in the whole boundary layer. Research on TKE should concentrate on trying to understand the statistical properties of turbulence. Due to the complex nonlinear nature of the atmosphere, unresolved scales can fundamentally influence the resolved larger scales. Since explicitly characterizing the unresolved processes in not feasible, the statistics need to be parameterized as a function of the unresolved flow (Teixeira et al., 2008). According to MOST, the TKE after its nondimensionalization by the friction velocity will follow the 1/3 power law

$$e/u_*^2 = \begin{cases} a_1(1-bZ/L)^{1/3} & z/L < 0 \\ a_1(1+cZ/L)^{1/3} & z/L > 0 \end{cases}$$

(here, e is TKE and u_* is the friction velocity).

Figure 8 shows the scatter relationship between the dimensionless TKE of the dominant wind direction and the atmospheric stability of the study area. Equations (7) and (8) are the optimal functions of the TKE in the southeast and west-northwest directions:

$$e/u_*^2 = \begin{cases} 11.1(1-20Z/L)^{1/3} & z/L < 0 \\ 11.1(1+92Z/L)^{1/3} & z/L > 0 \end{cases}; \quad (7)$$

$$e/u_*^2 = \begin{cases} 10.5(1-28Z/L)^{1/3} & z/L < 0 \\ 10.5(1+137Z/L)^{1/3} & z/L > 0 \end{cases}. \quad (8)$$

It can be seen that dimensionless TKE of the near-surface at Dingxi follows MOST under convective and stable conditions. Notably, the values of the dimensionless turbulence intensity of the two prevailing wind directions are close to one another under neutral conditions, and the values are 11.1 and 10.5, respectively. Even when compared with the result of 12.85 for a city suburb under neutral conditions (Niu et al., 2012), the difference is relatively small, indicating that the constant coefficient a has certain universality. However, the differences between b and c values are relatively large, which reflects the effects of the heterogeneity of the near-surface on the turbulence intensity (Yue et al., 2010).

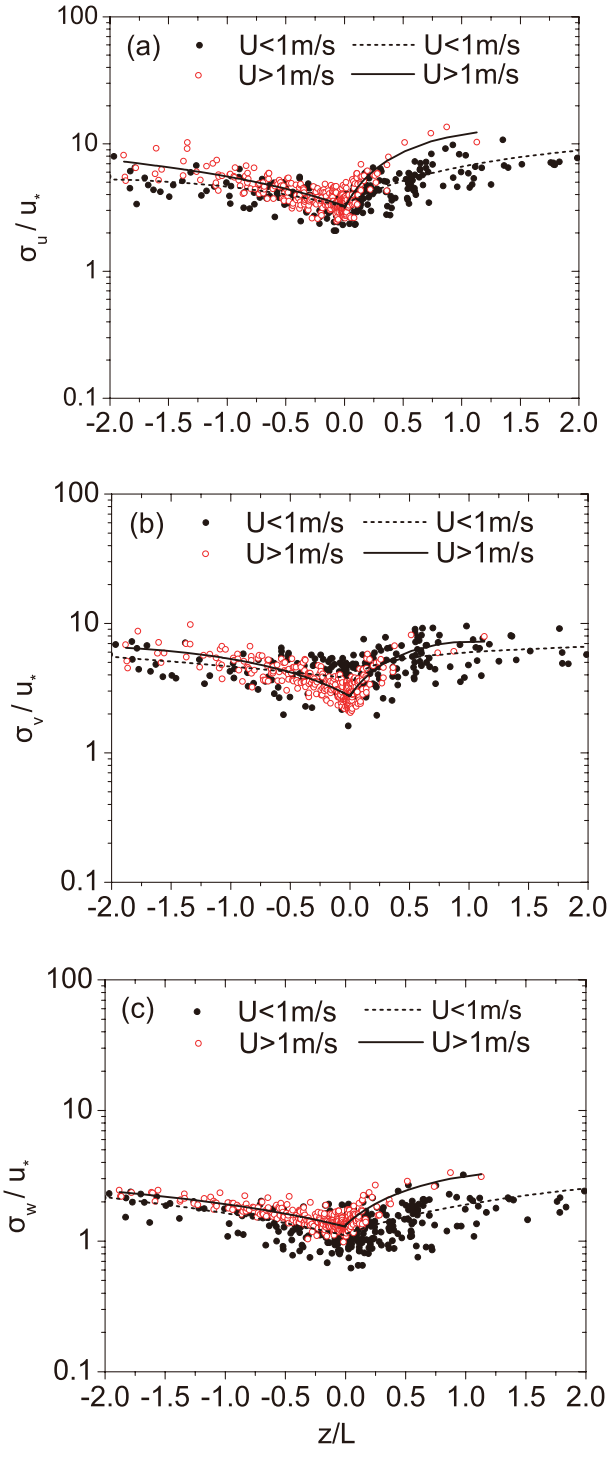

Fig. 6. Variations of σ_u/u_*, σ_v/u_* and σ_w/u_* with stability in the southeast direction.

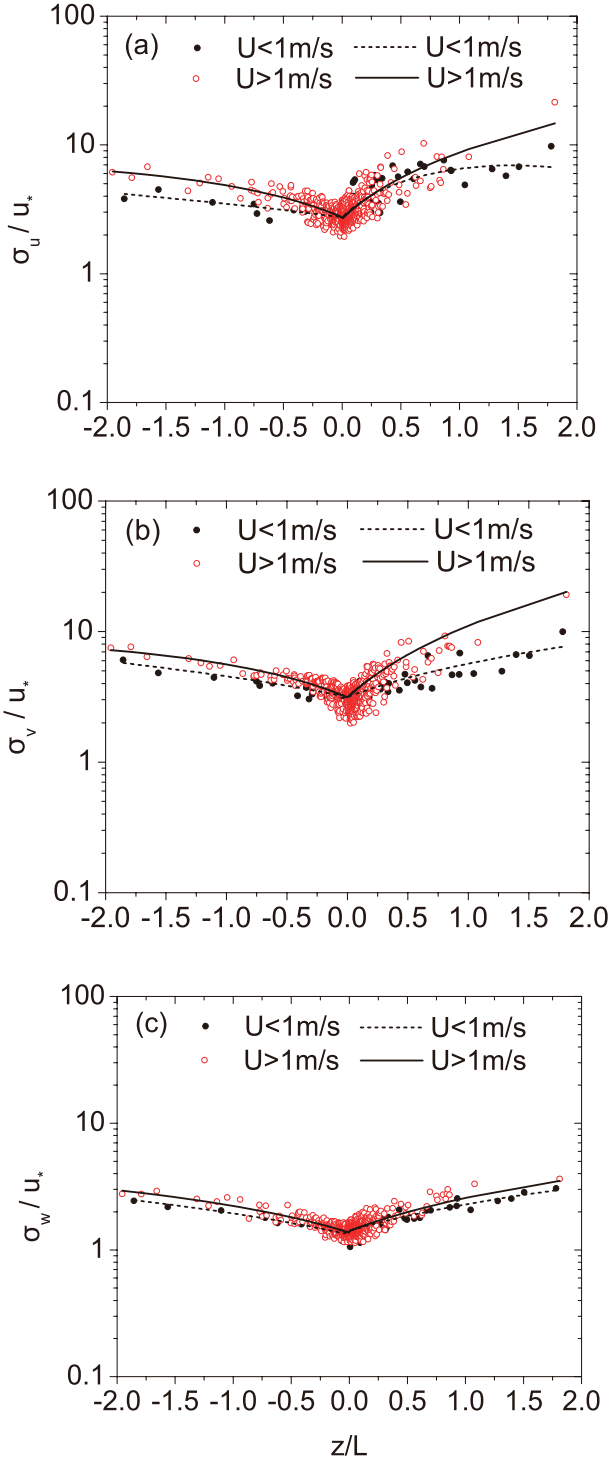

Fig. 7. Variations of σ_u/u_*, σ_v/u_* and σ_w/u_* with stability in the west-northwest direction.

3.4. *Contribution of the shear effect and buoyancy on TKE*

Each item of the TKE budget equation describes a different part of the physical process of turbulent formation except the turbulence dissipation rate. Comparing the interactions among these parts helps to determine the ability of the airflow to maintain or change the turbulence flow. The coordinate system is selected to be consistent with the average wind direction. When assuming that the horizontal direction is uniform, and descent is ignored, a simplified form of the TKE equation can be obtained as

$$\frac{\partial e}{\partial t} = -\frac{g\overline{w'T_v'}}{T_v} - \overline{u'w'}\frac{\partial U}{\partial z} - \frac{\partial(\overline{w'e})}{\partial z} - \frac{1}{\rho}\frac{\partial(\overline{w'p'})}{\partial z} - \varepsilon, \quad (9)$$

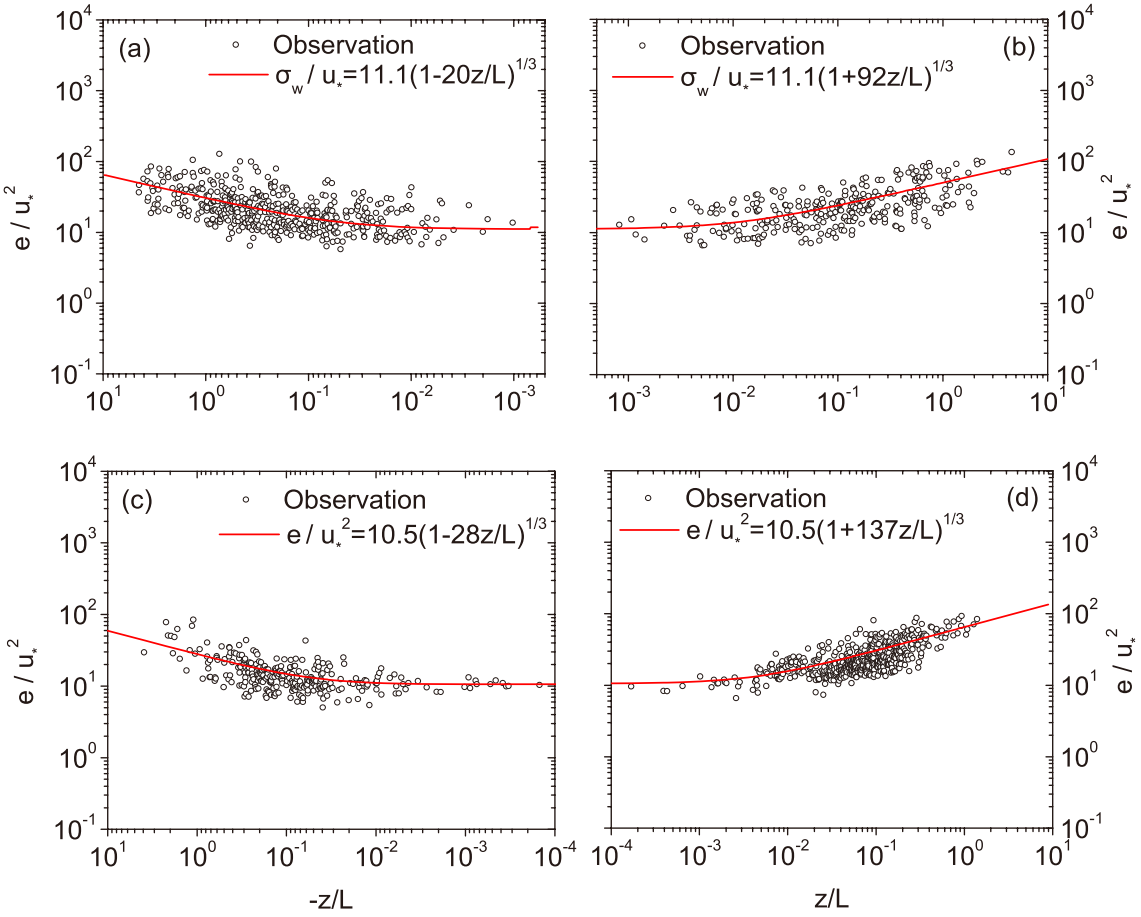

Fig. 8. Changes of TKE with stability: (a, b) southeast direction; (c, d) west-northwest direction.

where e is TKE, t is time, g is acceleration due to gravity, T_v is virtual temperature, $\overline{w'T_v'}$ is turbulent heat flux, $\overline{u'w'}$ is turbulent momentum, ρ is the air density, U is the wind speed, z is the observational height, w' is the vertical velocity fluctuation, P' is the atmospheric pressure pulsation, and ε is the turbulence dissipation rate. In Eq. (9), the first item on the right represents the production of buoyancy, or the consumption item, which is determined by the vertical transmission direction of the heat flux. The second item represents the production of mechanical shear, or the loss item. The third item represents the turbulence transport of TKE. The fourth item comprises pressure-related quantities, which is often associated with oscillations in the atmosphere. The fifth item is the viscous dissipation of TKE, and as long as TKE is not zero, it is always the loss item.

When the stratification is unstable, there is a good correlation between TKE and mechanical shear and buoyancy effects (Figs. 9a and b). Under conditions of significant levels of 0.1‰ the fitting relationship equations in the southeast direction are

$$e = 3.681\left(\overline{u'w'}\frac{\partial U}{\partial z}\right)^{0.303} \quad (R^2 = 0.645)$$

and

$$e = 3.683\left(\frac{g\overline{w'T_v'}}{T_v}\right)^{0.303} \quad (R^2 = 0.645)\,,$$

respectively. In the west-northwest direction, the fitting formulas are

$$e = 4.737\left(\overline{u'w'}\frac{\partial U}{\partial z}\right)^{0.415} \quad (R^2 = 0.543)$$

and

$$e = 1.387\left(\frac{g\overline{w'T_v'}}{T_v}\right)^{0.161} \quad (R^2 = 0.376)\,,$$

respectively. When the atmospheric stratification is stable, the relationship between TKE and $\overline{u'w'}(\partial U/\partial z)$ still meets the power function relationship, and there is a good correlation (Figs. 9e and g). Under conditions of a significant level (0.1‰, the fitting formula in the southeast direction is

$$e = 1.068\left(\overline{u'w'}\frac{\partial U}{\partial z}\right)^{0.258} \quad (R^2 = 0.580)\,.$$

The fitting formula in the west-northwest direction is

$$e = 1.982\left(\overline{u'w'}\frac{\partial U}{\partial z}\right)^{0.331} \quad (R^2 = 0.599)\,.$$

However, there is almost no correlation between TKE and $(g\overline{w'T_v'}/T_v)$ (Figs. 9f and h). During the present study period, the shearing effect of wind speed in the research area is strong, and so the shearing effects of airflow could enhance turbulence under all stability conditions. The surface

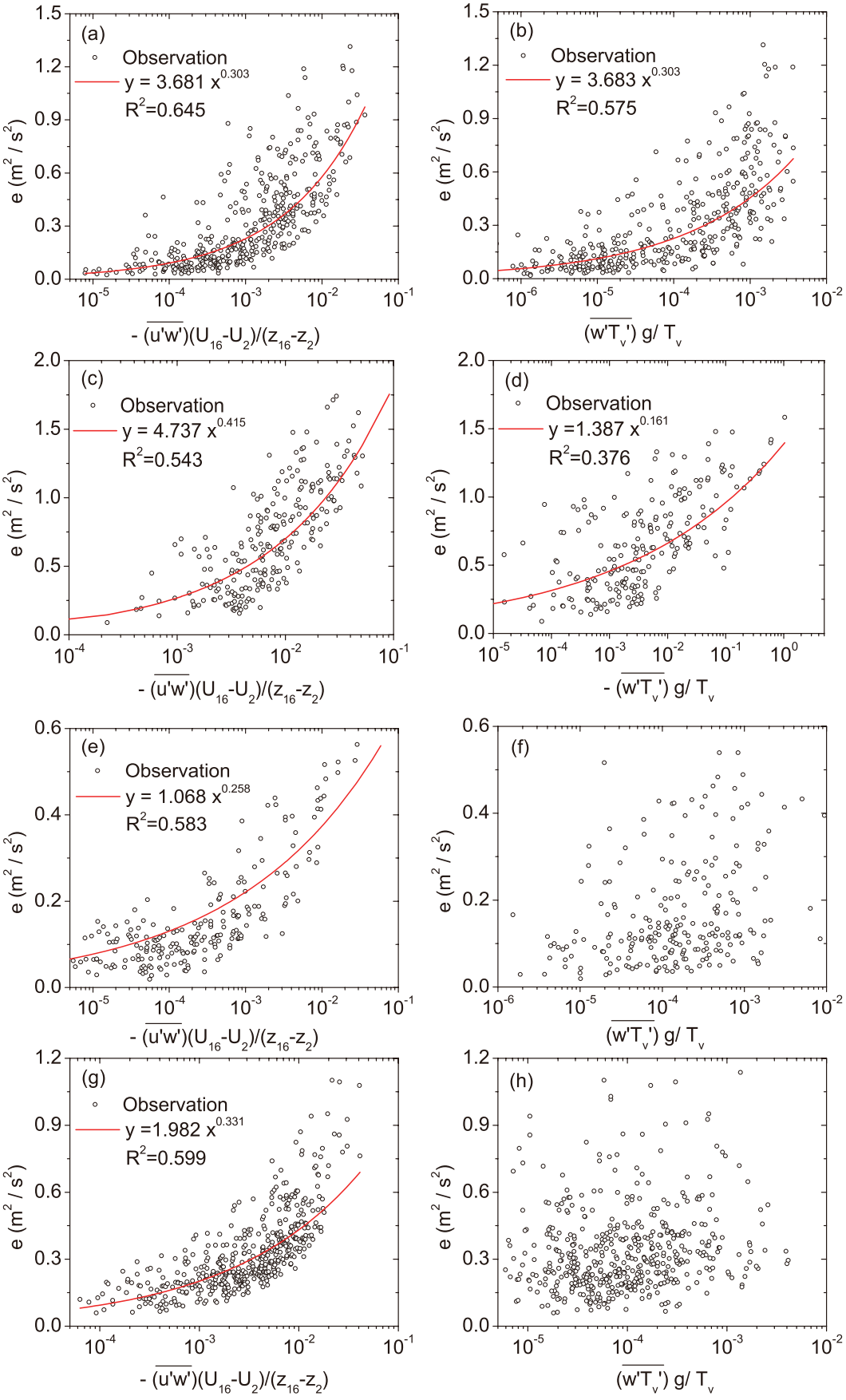

Fig. 9. Relationships between $\overline{u'w'}\frac{\partial U}{\partial z}$, $\frac{g\overline{w'T_v'}}{T_v}$ and TKE.

temperature during the daytime is relatively low, for unstable conditions, and the buoyancy and shear effect of wind speed together constitute the production items of TKE. At night, the ground temperature is lower than the air temperature, for stable conditions, the contribution of buoyancy to TKE is relatively small, and the mechanical shear becomes almost the only production item of turbulence (Clark et al., 2004).

4. Conclusions

Turbulent transport is one of the basic characteristics of the atmospheric boundary layer. Detailed knowledge of turbulence characteristics is important for understanding atmospheric phenomena, especially over heterogeneous terrain. Turbulence intensity and TKE parameters are beneficial for describing the exchange of properties between the surface and atmosphere effectively.

In this study, the standard deviations of velocities over the heterogeneous terrain of Dingxi are calculated for a valley region with the data for December 2003 to January 2004, and classified according to the wind direction and wind speed. The TKE is then also classified according to the wind direction. The applicability of MOST is investigated, and the results indicate that the normalized standard deviation of velocity fluctuations and TKE follow similar rules for the two prevailing wind directions. The ratio of σ_w/u_* is 1.3 and 1.4 in the southeast and west-northwest directions, respectively, and the values are close to those of flat terrain under neutral conditions. However, σ_u/u_* and σ_v/u_* are 3.7 and 3.3 in southeast direction, and 2.9 and 3.2 in west-northwest direction, respectively. The values of dimensionless turbulence intensity in the southeast and west-northwest directions under neutral conditions are 11.1 and 10.5, respectively.

Close correlation is found among the variances of σ_u/u_*, σ_v/u_* and σ_w/u_* with z/L over the Dingxi site under different wind speed conditions, for all stability conditions. The decreasing trend of the ratio with z/L increases more significantly under the conditions of high speed wind than low speed wind for unstable conditions. Under stable conditions, the increasing trend of the ratio with z/L increases slightly more under the conditions of high speed wind than low speed wind.

Whether or not the conditions of stratification are stable, the shear effect of airflow enhances the turbulence, because the shear effect of the wind speed in winter over the Loess Plateau is strong. In the daytime, the buoyancy and shear effect of wind speed together constitute the production items of TKE under unstable stratification. At night, the mechanical shear becomes almost the only production form of turbulence.

Acknowledgements. This work was supported by the National Basic Research Program of China (Grant No. 2012CB955304), the National Natural Science Foundation of China (Grant Nos. 41075008 and 40830957), the Special Financial Grant of China Postdoctoral Science Foundation (Grant No. 2013T60901), the Arid Meteorology Foundation of the Institute of Arid Meteorology of the China Meteorological Administration (Grant No. IAM201408), and the Ten Talents Program of Gansu Meteorology Bureau.

REFERENCES

Acevedo, O. C., O. L. L. Moares, R. da Silva, V. Anabor, D. P. Bittencourt, H. R. Zinermann, R. O. Magnago, and G. A. Degrazia, 2007: Surface-to-atmosphere exchange in a river valley environment. *J. Appl. Meteor.*, **46**, 1169–1181.

Al-Jiboori, M. H., Y. M. Xu, and Y. F. Qian, 2001: Turbulence characteristics over complex terrain in west China. *Bound.-Layer Meteor.*, **101**, 109–126.

Andreas, E. L., and B. B. Hicks, 2000: Comments on "Critical test of the validity of Monin- Obukhov similarity during convective conditions". *J. Atmos. Sci.*, **59**, 2605–2607.

Anfossi, D., D. Oettl, G. Degrazia, and A. Goulart, 2005: An analysis of sonic anemometer observations in low wind speed conditions. *Bound.-Layer Meteor.*, **114**, 179–203.

Businger, J. A., J. C. Wyngaard, Y. Izumi, and E. F. Bradley, 1971: Flux–profile relationships in the atmospheric surface layer. *J. Atmos. Sci.*, **28**, 181–189.

Clark, I., P. Assamoi, J. Bertrand, and F. Giorgi, 2004: Characterization of potential zones of dust generation at eleven stations in the southern Sahara. *Theor. Appl. Climatol.*, **77**, 173–184.

Founda, D, M. Tombrou, D. P. Lalas, and D. N. Asimakopoulos, 1997: Some measurements of turbulence characteristics over complex terrain. *Bound.-Layer Meteor.*, **83**, 221–245.

Hammerle, A., A. Haslwanter, M. Schmitt, M. Buhn, U. Tappeiner, A Cernusca, and G. Wohlfahet, 2007: Eddy covariance measurements of carbon dioxide, latent and sensible energy fluxes above a meadow on a mountain slope. *Bound.-Layer Meteor.*, **122**, 397–416.

Huang, J. P., and Coauthors, 2008: An overview of the semi-arid climate and environment research observatory over the Loess Plateau. *Adv. Atmos. Sci.*, **25**(6), 906–921, doi: 10.1007/s00376-008-0906-7.

Kaimal, J. C., 1973: Turbulence spectra, length scales and structure parameters in the stable surface layer. *Bound.-Layer Meteor.*, **4**, 289–309.

Liu, H. Z., Z. X. Hong, H. S. Zhang, J. Y. Chen, F. Hu, and H. Y. Chen, 2003: The turbulent characteristics in the surface layer over dune at Naiman in Inner Mongolia. *Chinese Journal of Atmospheric Sciences*, **27**(3), 389–398. (in Chinese)

Li, J., S. H. Liu, H. P. Liu, J. Chan, A. Y. S. Cheng, F. Hu, and H. Z. Liu, 2003: Surface imbalance energy calculated and analyzed with the data of EBEX-2000. *Acta Meteorologica Sinica*, **17**, 448–464.

Liu, L., T. J. Wang, Z. H. Sun, Q. J. Wang, B. L. Zhuang, Y. Han, and S. Li, 2012: Eddy covariance tilt corrections over a coastal mountain area in South-east China: Significance for near-surface turbulence characteristics. *Adv. Atmos. Sci.*, **29**(6), 1264–1278, doi: 10.1007/s00376-012-1052-9.

Louis, J. F. 1979: A parametric model of vertical eddy fluxes in the atmosphere. *Bound.-Layer Meteor.* **17**, 187–202.

Ma, Y. M., W. Q. Ma, Z. Y. Hu, M. S. Li, J. M. Wang, H. Ishikawa, and O. Tsukamoto, 2002: Similarity analysis of atmospheric turbulent intensity over grassland surface of Qinghai-Xizang plateau. *Plateau Meteorology*, **21**, 514–517. (in Chinese)

Mahrt, L., 2007: Weak-wind mesoscale meandering in the nocturnal boundary layer. *Enviro. Fluid Mech.*, **7**, 331–347.

Mahrt, L., 2010: Variability and maintenance of turbulence in the

very stable boundary. *Bound.-Layer Meteor.*, **135**, 1–18.

Mahrt, L., J. J Sun, W. Blumen, T. Delany, and S. Oncley, 1998: Nocturnal boundary-layer regimes. *Bound.-Layer Meteor.*, **88**, 255–278.

Massman, W. J., and X. Lee, 2002: Eddy covariance flux corrections and uncertainties in long-term studies of carbon and energy exchanges. *Agricultural and Forest Meteorology*, **113**, 121–144.

Martins, C. A., L. L. Osvaldo, O. C. Acevedo, and G. A. Degrazia, 2009: Turbulence intensity parameters over a very complex terrain. *Bound.-Layer Meteor.*, **133**, 35–45.

Monin, A. S., and A. M. Yaglom, 1971: Statistical fluid mechanics, Vol 1. The MIT Press, Cambridge, Mass, 769 pp.

Moraes, O. L. L., Acevedo, O. C. Degrazia, G. A., Anfossi, D., Da Siliva, R., Anabor, V, 2005: Surface layer turbulence parameters over a complex terrain. *Atmos. Eviron.*, **39**, 3103–3112.

Moraes, O. L. L., 2000: Turbulence characteristics in the surface boundary layer over the South American Pampa. *Bound.-Layer Meteor.*, **96**, 317–335.

Muschinski, A., R. G. Frehlich, and B. B. Balsley, 2004: Small-scale and large-scale intermittency in the nocturnal boundary layer and the residual layer. *J. Fluid Mech.*, **515**, 319–351.

Nieuwstadt, F. T. M., 1984: The turbulent structure of the stable, nocturnal boundary layer. *J. Atmos. Sci.*, **41**, 2202–2216.

Niu, S. J., L. J. Zhao, C. S. Lu, J. Yang, J. Wang, and W. W. Wang, 2012: Observational evidence for the Monin-Obukhov similarity under all stability conditions. *Adv. Atmos. Sci.*, **29**(2), 285–294, doi: 10.1007/s00376-011-1112-6.

Panofsky, H. A., and R. A. McCormick, 1960: The spectrum of vertical velocity near the surface. *Quart. J. Roy. Meteor. Soc.*, **86**, 495–503.

Panofsky, H. A., and J. A. Dutton, 1984: *Atmospheric Turbulence*. Wiley, New York, 397 pp.

Panofsky, H. A., H. Tennekes, D. H. Lenschow, and J. C. Wyngaard, 1977: The characteristics of turbulent velocity components in the surface layer under convective conditions. *Bound.-Layer Meteor.*, **11**, 355–361.

Powell, M. D., P. J. Vickery, and T. A. Reinhold, 2003: Reduced drag coefficient for high wind speeds in tropical cyclones. *Nature*, **422**, 279–283.

Schmid, H. P., H. B. Su, C. S. Vogel, and P. S. Curtis, 2003: Ecosystem–atmosphere exchange of carbon dioxide over a mixed hardwood forest in northern lower Michigan. *J. Geophys. Res.*, **108**(D14), 4417–4435, doi: 10.1029/2002JD 003011.

Schmid, H. P., 1994: Source areas for scalars and scalar fluxes. *Bound.-Layer Meteor.*, **67**, 293–318.

Smedman, A. S., 1988: Observations of a multi-level turbulence structure in a very stable atmospheric boundary layer. *Bound.-Layer Meteor.*, **44**, 231–253.

Song, X. Z., H. S. Zhang, J. Y. Chen, and S. U. Park, 2010: Flux-gradient relationships in the atmospheric surface layer over the Gobi desert in China. *Bound.-Layer Meteor.*, **134**, 487–498.

Sorbjan, Z., 1987: An examination of local similarity theory in the stably stratified boundary layer. *Bound.-Layer Meteor.*, **38**, 63–71.

Teixeira, J., and Coauthors, 2008: Parameterization of the atmospheric boundary layer: A view from just above the inversion. *Bull. Amer. Meteor. Soc.*, **89**, 453–458.

Vickers, D., and L. Mahrt, 1997: Quality control and flux sampling problems for tower and aircraft data. *J. Atmos. Oceanic Technol.*, **14**, 512–526.

Wilson, J. D., 2008: Monin-Obukhov functions for standard deviations of velocity. *Bound.-Layer Meteor.*, **129**, 353–369.

Yue, P., S. J. Niu, Y. Q. Hu, and Q. Zhang, 2010: Turbulent intensity and its similarity function over an Inner Mongolian grassland during spring. *Science China Earth Sciences*, **53**(5), 733–780.

Yue, P., Q. Zhang, S. J. Niu, J. H. Yang, S. Wang, J. Z. Zhang, and X. L. Liu, 2011: Statistical characteristic of atmospheric turbulence in clear and dust weather conditions in Inner Mongolian grassland during spring. *Plateau Meteorology*, **30**(5), 1180–1188. (in Chinese)

Yue, P., Y. H. Li, Q. Zhang, and L. Zhang, 2012: Surface Energy-Balance closure in a gully region of the Loess Plateau at SACOL on eastern Edge of Tibetan Plateau. *J. Meteor. Soc. Japan*, **90C**, 173–184.

Yue, P., Q. Zhang, Y. H. Li, R. Y. Wang, S. Wang, and X. Y. Sun, 2013: Bulk transfer coefficients of momentum and sensible heat over semiarid grassland surface and their parameterization scheme. *Acta Physica Sinica*, **62**, 099202-1–9. (in Chinese)

Zeri, M., and L. D. A. Sá, 2011: Horizontal and vertical turbulent fluxes forced by a gravity wave event in the nocturnal atmospheric surface layer over the Amazon forest. *Bound.-Layer Meteor.*, **138**, 413–431.

Zhang, H. S., J. Y. Chen, and S. U. Park, 2001: Turbulence structure in unstable conditions over various surfaces. *Bound.-Layer Meteor.*, **100**, 243–261.

Zhang, Q., T. Yao, P. Yue, L. Y. Zhang, and J. Zeng, 2013: The influences of thermodynamic characteristics on aerodynamic roughness length over land surface. *Acta Meteorologica Sinica*, **27**(2), 249–262.

Zuo, J. Q., J. P. Huang, J. M. Wang, W. Zhang, J. R. Bi, G. Y. Wang, W. J. Li, and P. J. Fu, 2009: Surface turbulent flux measurements over the Loess Plateau for a semi-arid climate change study. *Adv. Atmos. Sci.*, **24**(4), 679–691, doi: 10.1007/s00376-009-8188-2.